scientific reports

Check for updates

OPEN

TNF-α inhibits Epstein Barr virus reactivation through the GPX4 mediated glutathione pathway

Youyu Zhang[1,4], Yilin Wu[1,4], Beining Ding[1], Qian Li[1], Xuenuo Chen[1], Huiling Liu[1], Mingyan Xu[2], Yinghua Lan[3]✉ & Yongguo Li[1]✉

Epstein–Barr virus (EBV) is a carcinogenic γ-herpesvirus that remains latent in more than 95% of adults. The virus can undergo lytic activation when immune function is suppressed or when stimulated by drugs or pathogens. EBV reactivation poses a significant threat to human health and is closely associated with various cancers, such as Burkitt's lymphoma and nasopharyngeal carcinoma. Inhibiting EBV reactivation is a current clinical challenge. Tumour necrosis factor-α (TNF-α), an important cytokine, has different effects on various viruses. It also exerts varying effects on the same virus depending on the type of infected cell. This study aimed to investigate the impact of TNF-α on EBV reactivation and its underlying mechanisms. Our experimental research revealed that TNF-α significantly inhibits EBV reactivation and that this inhibitory effect is mediated primarily through its receptor TNFR1. Furthermore, TNF-α affects the expression of the GPX4 protein and regulates the potential ferroptosis state of cells. Using transmission electron microscopy and other methods, we observed typical characteristics of ferroptosis, such as changes in mitochondrial morphology and Fe2 + accumulation. Additionally, we established stable GPX4-knockdown cell lines, which demonstrated the crucial role of GPX4 in the process of TNF-α-mediated inhibition of EBV reactivation. Overall, TNF-α acts on the TNFR1 receptor, thereby affecting the GPX4 protein and the ferroptosis pathway to achieve its inhibitory effect on EBV reactivation. These findings provide new insights into the mechanisms of EBV reactivation and may offer new perspectives for the early treatment of EBV-related diseases.

Keywords TNF-α, EBV reactivation, Ferroptosis, GPX4

Epstein–Barr virus (EBV) is an oncogenic γ-herpesvirus virus containing 172 kb of double-stranded linear DNA that was originally identified in 1964 in patients with Burkitt's lymphoma (BL)[1]. EBV infects its primary host target, human B cells, by binding to complement 47 receptors 1 and 2 and MHC class II[2]. It continues to infect more than 95% of the adult population worldwide[3]. Primary EBV infections are usually asymptomatic, occur in childhood, and are then carried in the body for life[4]. EBV infection can lead to a variety of diseases. During adolescence or adulthood, 30–50% of infections manifest as infectious mononucleosis (IM)[1]. Globally, EBV causes more than 200,000 cancers annually, including endemic Burkitt's lymphoma, Hodgkin's lymphoma, non-Hodgkin's lymphoma, central nervous system (CNS) lymphoma in patients with late-stage HIV infection, posttransplant lymphoproliferative disease (PTLD), nasopharyngeal carcinoma, and gastric carcinoma [5]. Therefore, further research on the EBV is highly important for human health.

Latency and reactivation are hallmarks of herpesvirus infection. In almost all EBV-infected B cells, viral infection exists in a latent state. In latent infection, the virus is unable to replicate to produce infectious zygotic virus particles, and the genes expressed in latent EBV infection encode eight EBV proteins, two untranslated EBV-encoded small RNAs (EBERs), 25 premicroRNAs, Epstein–Barr nuclear antigen 1 (EBNA1), and two latent membrane proteins (LMP1 and LMP2)[7]. The expression of these genes during the latency period ensures that EBV-infected B cells survive the germinal centre response, thus establishing a lifelong latent infection within the host lymphoid tissue[8]. In the normal immune environment, latent EBV and the immune system are maintained in a state of equilibrium and when the body's immune function declines or is exposed to external irritants. In

[1]Department of Infectious Diseases, The First Affiliated Hospital of Chongqing Medical University, Chongqing 400016, China. [2]Department of Infectious Diseases, The First Affiliated Hospital of Harbin Medical University, Harbin 150001, China. [3]Department of Infectious Diseases, The Second Affiliated Hospital of Chongqing Medical University, Chongqing 400016, China. [4]Youyu Zhang and Yilin Wu are contributed equally to this work. ✉email: lan_yinghua@163.com; liyongguodoctor@163.com

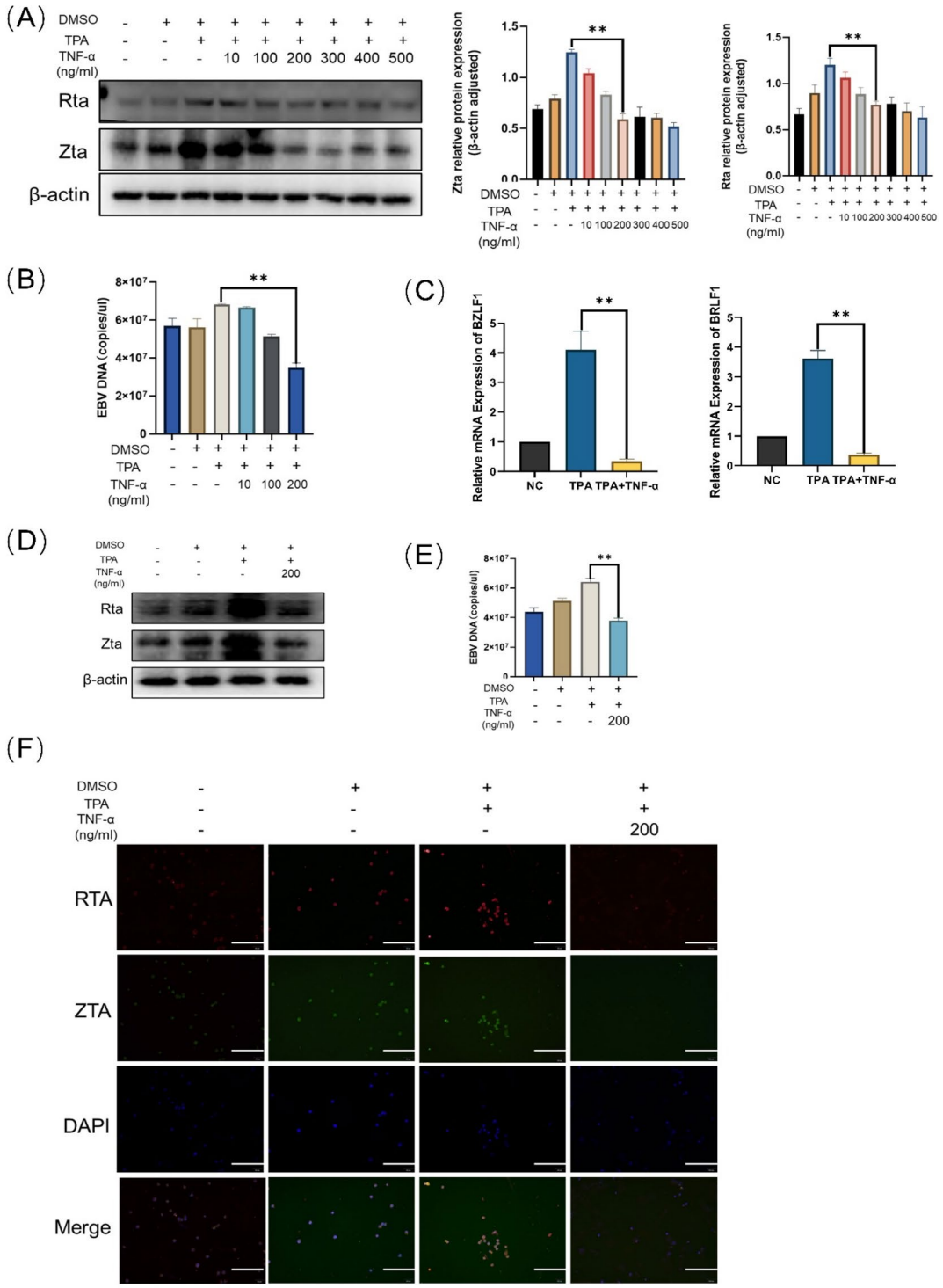

addition, EBV reactivation has been demonstrated to occur in a wide range of autoimmune disease disorders and immunocompromised individuals, such as those receiving immunosuppressive therapy or those with AIDS[4] or COVID-19, which can lead to EBV reactivation[9]. Stimulation with drugs such as HDACIs[10], bendamustine[11] and aspirin[12] can also reactivate EBV, leading to the production of infectious viral particles that allow the virus to spread from cell to cell and from host to host. When latent EBV reactivates and enters the lysogenetic phase, it causes the acute symptoms of infection once again[13]. In the lytic infection state, the virus can undergo complete gene replication and express viral proteins[14]. This further highlights the urgent need to study the mechanism of EBV reactivation.

The key to the initiation of EBV lysogenic replication is the expression of immediate early genes (IEs), including BZLF1 (Zta)[15] and BRLF1 (Rta)[16]. These two IE proteins are the switches of the lysis phase, switching on the entire viral replication cascade. It has been shown that reactive oxygen species (ROS) can mediate

◀**Fig. 1**. TNF-α inhibits EBV reactivation in vitro. (A) Raji cells were treated with TPA (20 ng/ml) and different concentrations of TNF-α for 24 h. Western blotting was performed with the indicated antibodies. (B) EBV DNA was extracted from Raji cells treated with TPA (20 ng/ml) or different concentrations of TNF-α, and the EBV DNA concentration was measured by digital PCR. (C) RNA was extracted from Raji cells treated with TPA (20 ng/ml) or TNF-α (200 ng/ml), and the mRNA expression levels of the EBV genes BRLF1 and BZLF1 were measured by real-time PCR. (D) LCL cells were treated with TPA (20 ng/ml) and different concentrations of TNF-α for 24 h. Western blotting was performed with the indicated antibodies. (E) EBV DNA was extracted from LCL cells treated with TPA (20 ng/ml) or TNF-α (200 ng/ml), and the EBV DNA concentration was measured by digital PCR. (F) Raji cells were induced with TPA (20 ng/ml) and TNF-α (200 ng/ml) for 24 h and harvested for immunofluorescence assays with Rta (red) and Zta (green) antibodies. The data shown are representative of three independent experiments. The data are presented as the means ± SDs. $^{*}P < 0.05$; $^{**}p < 0.01$ by one-way ANOVA.

reactivation of EBV with the activated promoter Rta[17]. Similarly, both fungal metabolites[18] and chemicals[19] can lead to EBV reactivation via ROS production accompanied by activation of the Zta, Rta promoter. The latest research suggests a link between ferroptosis and EBV reactivation[20]. Distinct from other forms of regulated cell death, such as necrosis, apoptosis or autophagy, ferroptosis has unique morphological, biochemical, genetic and immunological features[21]. Ferroptosis is an iron-dependent lipid peroxidation and ROS-induced programmed cell death (PCD) modality that relies on iron-mediated oxidative damage, increased iron accumulation, and free radical production, and a fatty acid supply with increased lipid peroxidation is critical for the induction of ferroptosis[22]. Ferroptosis is regulated mainly by the GSH/GPX4 pathway[23]. How to inhibit EBV reactivation by regulating the potential ferroptotic state and ROS still needs to be further investigated.

Studies have shown that cytokines are involved in viral replication. For example, IL-27 can inhibit the replication of many viruses[24], and IL-4 can promote viral replication[25]. Tumour necrosis factor (TNF-α) plays a crucial role in both normal and tumour cells and is a widely studied cytokine[26]. TNF-α plays an important roles in many processes, such as cell survival, apoptosis, necrosis, and intercellular communication[27]. TNF-α, a pleiotropic cytokine, exists in two biologically active forms: transmembrane TNF-α (TMTNF-α) and secretory TNF-α (STNF-α). STNF-α is biologically active as a homotrimer and acts through binding to the TNFR1 receptor. Studies have shown that Streptococcus haematobium can be activated by triggering the host tumour necrosis factor-α (TNF-a) cell signalling pathway[28], but the influence of the addition of TNF-α alone on EBV reactivation is still unknown. Therefore, further investigation of the effect of TNF-α on EBV reactivation and its specific mechanism is highly clinically important.

TNF-α has no direct effect on apoptosis in EBV-positive cell lines[29]. However, more than a decade ago, multiple modes of cell death associated with TNF-α were shown to involve ROS[30]. This link between TNF-α and ROS adds another dimension of complexity to the TNF signalling network, as ROS act on numerous proteins required for the regulation of cellular homeostasis, including proteins that mediate cell proliferation, survival, death, differentiation, DNA repair and metabolism [30]. Notably, oxidative stress plays a key role in mediating EBV reactivation, as LMP1, an EBV-encoded protein, promotes EBV reactivation by generating ROS[29]. This finding provides significant clues to further reveal the mechanism of EBV reactivation, which is of potential clinical value for gaining insights into the early diagnosis and treatment of EBV-associated diseases.

The aim of this study was to explore the effect of TNF-α on EBV reactivation and its specific mechanism to further elucidate how cytokines affect EBV reactivation and to explore therapeutic methods for early intervention in EBV-related diseases. We experimentally and logically demonstrated that TNF-α can influence EBV reactivation by affecting the GPX4 protein and influencing the potential ferroptosis state of cells. This study will help establish a cytokine network system and open new avenues for the clinical treatment of EBV-related diseases, especially Burkitt's lymphoma (EBV latent infection).

Results

TNF-α inhibits EBV reactivation by acting on the TNFR1 receptor

In our previous studies, we demonstrated that gram-negative bacterial LPS can mediate EBV reactivation through inflammatory factor storms and that TNF-α is a key factor in this process. We first performed ELISA to detect the secretion of endogenous TNF-α in two cell lines, LCL and Raji. The results were consistent with those of Miyauchi et al. (2011)[32] (Supplementary Fig. 1). To further investigate the role of TNF-α in EBV reactivation, we used TPA, a positive inducer of EBV, to stimulate Raji cells, which are in the latent state of EBV infection. Raji cells were stimulated with TPA (20 ng/ml) for 24 h, and protein extracts were assayed after 24 h to reveal significant increases in Zta and Rta protein expression, indicating that the EBV infection changed from a latent state to a reactivated state. We then treated the reactivated Raji cells with several concentrations of TNF-α (10, 100, 200, 300, 400, and 500 ng/ml). Zta and Rta expression levels decreased in a concentration-dependent manner with the addition of TNF-α (Fig. 1A). The TNF-α concentration of 200 ng/ml had the best inhibitory effect. DNA extracted from Raji cells was used to assay viral titre, which revealed an inhibitory effect compared with that of the TPA-treated group (Fig. 1B). Moreover, RNA from Raji cells was extracted and tested to evaluate the expression of the immediate early genes BZLF1 and BRLF1. The results revealed that the mRNA expression levels of BZLF1 and BRLF1 were significantly lower than those of the TPA-treated samples (Fig. 1C). We subsequently used LCLs as a control for validation, and Zta and Rta protein expression levels decreased with the addition of TNF-α (Fig. 1D). Similarly, DNA extracted from LCL cells was used to assay viral titre, which yielded the same result (Fig. 1E). The results of the cytofluorescence analysis revealed that the fluorescence intensities of the Zta and Rta proteins were significantly weaker than those of the TPA-treated group (Fig. 1F),

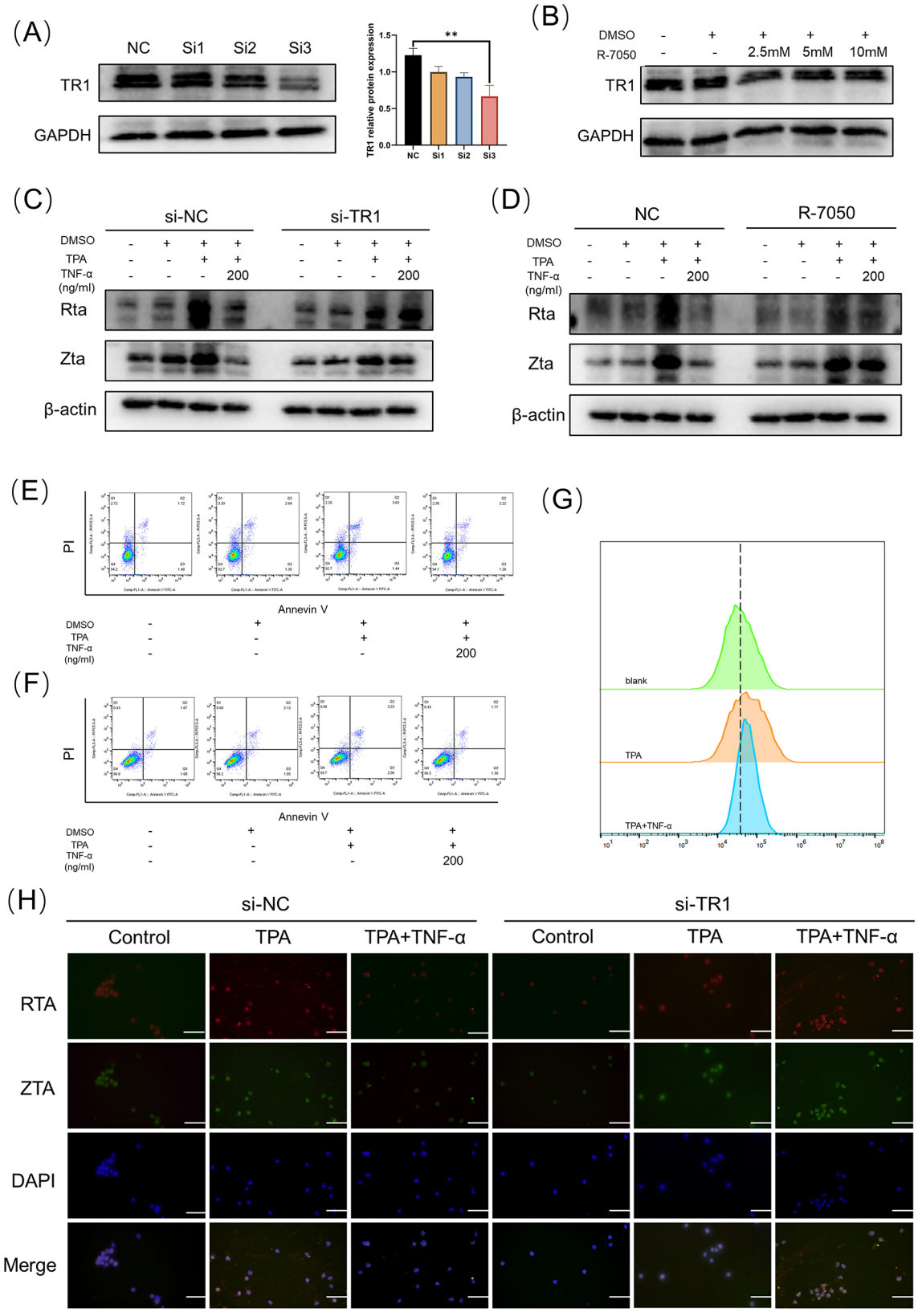

which also verified our conclusion. The reactivation of both Raji cells and LCL cells with 200 ng/ml TNF-α effectively inhibited the replication and reactivation of the EBV infection.

To further validate the effect of TNF-α on EBV reactivation, TNFR1 small interfering RNA was used to knock down the expression of TNFR1, the main receptor of secretary TNF-α. After the TNFR1 receptor was knocked down by siRNA (Fig. 2A), In vehicle control groups, TNF-α exhibited inhibitory effects on Epstein-Barr virus (EBV) reactivation. However, under TNFR1 knockdown conditions, the expression levels of Rta and Zta in TNF-α-treated groups showed no significant reduction compared to positive controls, demonstrating that TNF-α lost

◀**Fig. 2**. TNF-α inhibits EBV reactivation by acting on TNFR1 receptors. (A) Raji cells were transfected with control (NC) siRNA or TNFR1 siRNA. The cell lysates were harvested, and western blotting was performed with TNFR1 antibodies. (B) Raji cells were directly treated with different concentrations of the TNFR1 inhibitor R-7050. The cell lysates were harvested, and western blotting was performed with the indicated antibodies. (C) After TNFR1 was knocked down with siRNA, the cells were treated with TPA (20 ng/ml) or TNF-α (200 ng/ml) for 24 h. The cell lysates were harvested, and western blotting was performed with the indicated antibodies. (D) After treatment with the TNFR1 inhibitor R-7050 (10 mM), Raji cells were induced with TPA (20 ng/ml) and TNF-α (200 ng/ml) for 24 h. The cell lysates were harvested, and western blotting was performed with the indicated antibodies. (E) For FC analysis of apoptosis, Raji cells were treated with TPA (20 ng/ml) or TNF-α (200 ng/ml) for 24 h. (F) For FC analysis of apoptosis, LCL cells were treated with TPA (20 ng/ml) or TNF-α (200 ng/ml) for 24 h. (G) The fluorescent ROS probe DCFH-DA was added to Raji cells treated with TPA (20 ng/ml) or TNF-α (200 ng/ml) for 24 h. (H) Raji cells were transfected with control (NC) siRNA or TNFR1 siRNA. After that, Raji cells were induced with TPA (20 ng/ml) and TNF-α (200 ng/ml) for 24 h and harvested for immunofluorescence assays using Rta (red) and Zta (green) antibodies. The data shown are representative of three independent experiments. The data are presented as the means ± SDs. $^{*}P < 0.05$; $^{**}p < 0.01$ by one-way ANOVA.

its suppressive effect on EBV reactivation when TNF-α/TNFR1 signaling was compromised(Fig. 2C). Compared with the TPA + TNF-α group, the fluorescence intensity of the si-NC-treated cells in the TPA-treated group was greater, but the fluorescence intensity of the si-TR1 cells was similar across the TPA + TNF-α group and TPA group(Fig. 2H). Moreover, we used the TNFR1 inhibitor R-7050 to verify that although the protein level of TNFR1 was not changed (Fig. 2B), we detected changes in the reactivation-related proteins Zta and Rta and found that the inhibition of EBV reactivation by TNF-α was significantly suppressed (Fig. 2D).

These results showed that TNF-α inhibited EBV reactivation in EBV-associated tumour cells, and the inhibitory effect of TNF-α on EBV reactivation was lost after inhibition of the TNFR1 receptor. These findings suggest that the inhibition of EBV reactivation by TNF-α is achieved by its primary receptor, TNFR1.

TNF-α inhibits EBV reactivation by affecting GPX4 protein expression

After confirming the ability of TNF-α to inhibit EBV reactivation, the possible mechanism by which TNF-α inhibits EBV reactivation needed to be further investigated. We first examined apoptosis in Raji cells by flow cytometry (Fig. 2E). Besides, LCL cells were examined apoptosis (Fig. 2F) which shows the similar result of Raji cells. As reported in other studies, flow cytometry revealed that TNF-α does not induce apoptosis in EBV-positive Burkitt's lymphoma cells[33], These findings prompted us to explore the relationship between the effects of TNF-α on cell survival and death and the effects on EBV reactivation. As previously described, ROS are strongly associated with EBV reactivation. Therefore, to explore the link between TNF-α and the ROS-dependent mode of cell death, the experimental groups were examined by flow cytometry, which revealed that TPA caused a marked increase in ROS, whereas 200 ng/ml TNF-α significantly reversed the increase in ROS (Fig. 2G). The EBV reactivation state is reportedly associated with susceptibility to ferroptosis, and TPA can exacerbate ferroptosis in SHSY5Y cells by increasing H_2O_2 levels[34]. This gave us a new idea: could TPA and TNF-α affect the potential ferroptosis state of cells?

To further investigate the mechanism by which TNF-α inhibits EBV reactivation, TMT proteomics were performed on Raji cells before and after TPA and TNF-α treatments to identify differentially expressed proteins and potential enrichment pathways, as shown in Fig. 3A. GPX4 is one of the major functional enzymes of glutathione peroxidase; it can eliminate peroxides and plays a key role in the anti-peroxidant defense system. After correlation analysis, the final key differential protein, GPX4, was verified by protein blotting. We treated Raji cells with TPA, and TNF-α and GPX4 protein and SLC7A11 protein expression levels decreased with the addition of TPA, and with the addition of TNF-α, GPX4 protein and SLC7A11 protein expression rebounded (Fig. 3C). The cell fluorescence results likewise confirmed that the GPX4 fluorescence intensity was attenuated after TPA stimulation compared with those in the control and TPA + TNF-α-treated groups (Fig. 3D), which is consistent with the TMT proteome sequencing results.

We then knocked down the GPX4 protein by lentiviral transduction to explore whether it could directly affect EBV reactivation. After successful transfection, we verified that sh-GPX4-2 had the best knockdown effect by WB (Supplementary Fig. 2)., and we then measured the expression levels of EBV reactivation-related proteins after stimulation with TPA and TNF-α in the control and experimental groups, respectively, using sh-NC and sh-GPX4-2. WB revealed that Rta and Zta protein expression levels were significantly greater in the sh-GPX4 group than in the sh-NC group (Fig. 3E). A viral titre assay revealed that after the GPX4 protein was knocked down, the inhibitory effect of TNF-α on EBV reactivation was significantly impaired (Fig. 3F). Moreover, RNA from sh-NC and sh-GPX4-2 cells were extracted and tested for the immediate early genes BZLF1 and BRLF1. The results revealed that in sh-GPX4-2 cells, the expression levels of the BZLF1 and BRLF1 mRNAs did not differ and were significantly greater than in the sh-NC cells (Fig. 3G). The results showed that the effect of TNF-α on EBV reactivation decreased with the reduction in GPX4 expression.

TNF-α inhibits the EBV reactivation state by affecting the classical pathway of GPX4-dependent ferroptosis

The key role of the GPX4 protein in the effect of TNF-α on EBV reactivation was identified. We found that the potentially enriched proteomic pathways included ferroptosis (Fig. 3B). To explore the role of TNF-α in the potential ferroptosis state of cells, we observed the typical morphological changes associated with ferroptosis

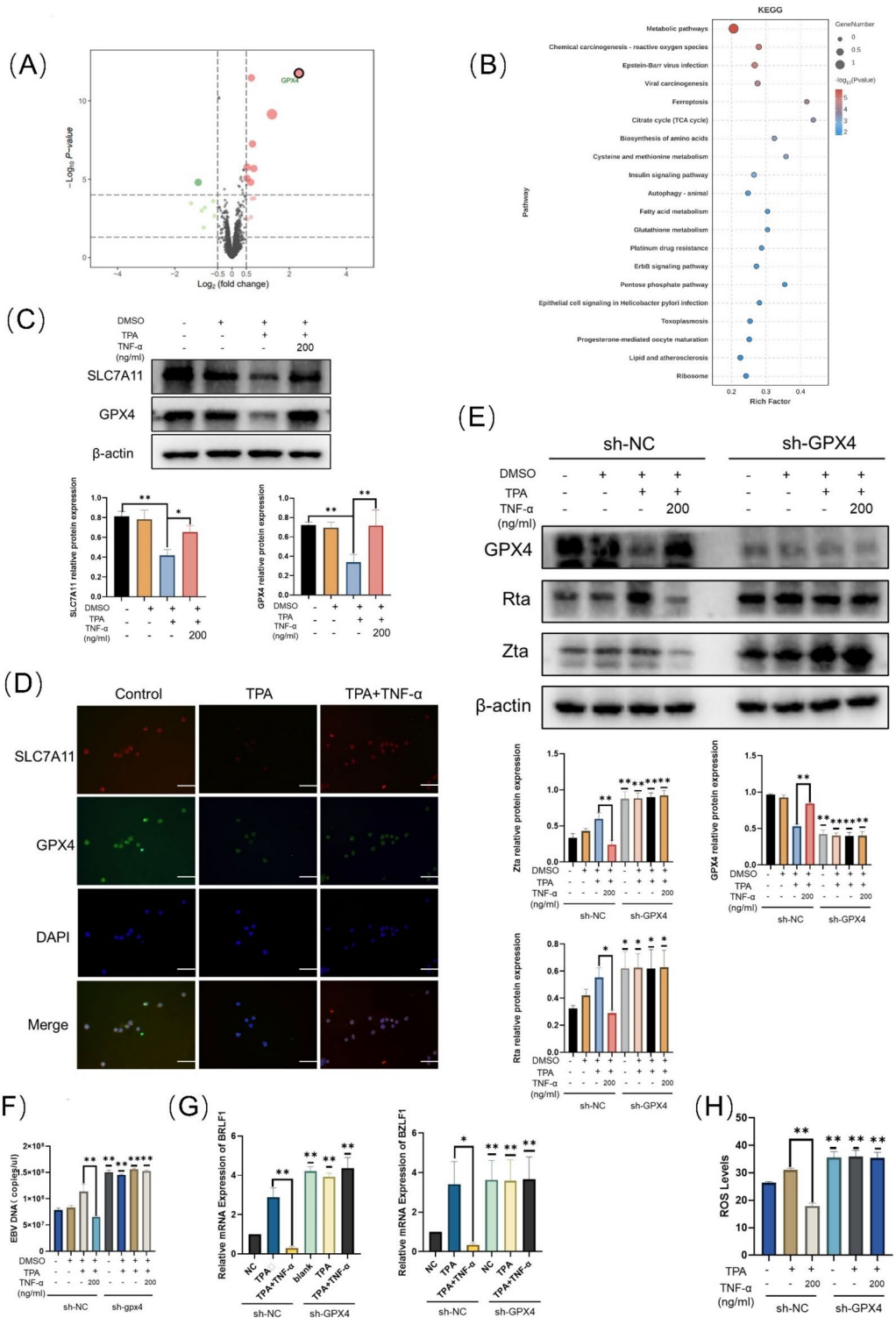

by transmission electron microscopy. The results suggested that the mitochondria in the blank group were morphologically more intact, with a rod-like morphology, surrounded by a double-layered membrane, with the inner membrane protruding inwards to form flat plate-like cristae, and that the cristae of the mitochondria were continuous. In contrast, in the group treated with TPA alone, the mitochondrial membrane became denser, the mitochondrial cristae were incomplete, the cristae were fractured, and the mitochondrial matrix became darker in colour. TPA caused mitochondrial crumpling, which was somewhat reversed by TNF-α (Fig. 4A). GPX4 is a key regulator of the classical pathway of the GSH–GPX4 ferroptosis pathway. Therefore, we aimed to explore the role of GPX4 in Raji cells. Given that GPX4 deficiency leads directly to cell death[35], we established stable GPX4 protein knockdown in Raji cells. We found that when cells were treated with the same concentration of TPA, GPX4 knockdown resulted in increased production of ROS (Fig. 3H) and MDA (Fig. 4B). Moreover, the effects of TNF-α were significantly impaired. GPX4 knockdown increases cellular sensitivity to oxidative stress. We

◀**Fig. 3**. TNF-α inhibits the EBV reactivation state by affecting GPX4 protein expression. (A) Volcano plot illustrating differentially expressed genes identified by TMT proteomics analysis between the TPA-treated group and the TPA + TNF-α group.Proteins upregulated and downregulated are shown in red and green, respectively. (B) Kyoto Encyclopedia of Genes and Genomes (KEGG) analysis of downregulated, upregulated, and total proteins in TMT proteomics. (C) Raji cells were treated with TPA (20 ng/ml) or TNF-α (200 ng/ml), and GPX4 and SLC7A11 expression was detected by WB. (D) Raji cells were induced with TPA (20 ng/ml) and TNF-α (200 ng/ml) and harvested for immunofluorescence assays using SLC7A11 (red) and GPX4 (green) antibodies. (E) After GPX4 protein expression was knocked down, Raji-shRNA-control and Raji-shRNA-hGPX4-2 cells were directly treated with TPA (20 ng/ml) or TNF-α (200 ng/ml) for 24 h. Cell lysates were harvested, and western blotting was performed with the indicated antibodies. (F) EBV DNA was extracted from Raji-shRNA-control and Raji-shRNA-hGPX4-2 cells treated with TPA (20 ng/ml) and TNF-α (200 ng/ml), and the EBV DNA concentration was measured by digital PCR. (G) RNA was extracted from Raji-shRNA-control and Raji-shRNA-hGPX4-2 cells treated with TPA (20 ng/ml) or TNF-α (200 ng/ml), and the mRNA expression levels of the EBV genes BRLF1 and BZLF1 were measured by real-time PCR. (H) The fluorescent ROS probe DCFH-DA was added to Raji-shRNA-control and Raji-shRNA-hGPX4-2 cells, which were treated with TPA (20 ng/ml) or TNF-α (200 ng/ml) for 24 h. The data shown are representative of three independent experiments. The data are presented as the means ± SDs. $^{*}P < 0.05$; $^{**}p < 0.01$ by one-way ANOVA.

also examined the GSH/GSSG ratio, which is correlated with GPX4 levels. The GSH/GSSG ratio of the sh-GPX4 group was lower than that of the sh-NC group, and the effects of TPA and TNF-α were significantly impaired (Fig. 4C). Compared with those in the sh-NC group, the intracellular Fe2 + levels were significantly increased (Fig. 4D). A fluorescence assay using Liperfluo revealed that GPX4 deficiency led to elevated lipid peroxide levels (Fig. 4E). These results suggest that decreased GPX4 expression decreases cellular tolerance to external oxidative stimuli, leading to EBV reactivation. Moreover, both TPA and TNF-α lose their original roles.

Ferroptosis activator (Erastin) and inhibitor (Fer-1) promote and suppress EBV reactivation

Our findings on in vitro experimental biological indicators, such as transmission electron microscopy, were consistent with ferroptosis. Owing to the complexity of ferroptosis and the lack of specific criteria and unique biomarkers of ferroptosis, we were unable to conclude that ferroptosis is involved in the mechanism of EBV reactivation. However, in addition to the above biological indicators, there are still basic criteria to demonstrate the involvement of ferroptosis, which should be inhibited by lipophilic antioxidants (e.g., ferrostatin-1 and lipstatin-1). Therefore, we treated Raji cells with Fer-1 after treatment with TPA. As a characteristic change in ferroptosis, morphological changes in mitochondria were observed by transmission electron microscopy (TEM). The administration of Fer-1 markedly prevented ultrastructural and morphological alterations in Raji cells, such as increased density of mitochondrial membranes and incomplete mitochondrial cristae, in Raji cells (Fig. 5A). Surprisingly, the protein expression levels of Zta and Rta also decreased with the addition of Fer-1 (Fig. 5B). These results were validated by PCR (Fig. 5E), which revealed that the potential ferroptosis state of the cells was correlated with the degree of EBV reactivation.

We then treated cells with Erastin to directly examine whether the occurrence of ferroptosis is associated with EBV reactivation. Ultrastructural analysis revealed that the mitochondrial ridge was reduced or absent and that rupture of the outer mitochondrial membrane (OMM) occurred in the Erastin-treated group and sh-GPX4 group(Fig. 5C). The occurrence of ferroptosis was first illustrated by electron microscopy, and then the Zta and Rta proteins were examined, the expression levels of which were greater than those in the control group (Fig. 5D). The expression levels of EBV reactivation-related proteins also increased with the addition of erastin. RNA samples from cells in this experiment were extracted and tested for the expression of the immediate early genes BZLF1 and BRLF1. The results revealed that the mRNA expression levels of BZLF1 and BRLF1 were significantly greater than those of the negative control group after treatment with erastin, which also validated the same conclusion (Fig. 5F).

In these experiments, we demonstrated that the exacerbation of ferroptosis leads to the occurrence of EBV reactivation and that the inhibition of ferroptosis can inhibit EBV reactivation to a certain extent.

Discussion

Epstein–Barr virus (EBV) was the first human-discovered oncogenic virus, and since its initial discovery in 1968, its threat to human health has become increasingly known[3]. The National Institutes of Health (NIH) has identified EBV control as critical for reducing the global cancer burden[36]. Disruption of the balance between the host and viral activation increases the risk of tumours. The results of previous studies suggest that EBV reactivation is an important risk factor for the development of EBV-associated diseases. Overall, the main roles of EBV reactivation are to induce genomic instability, counteract the host immune response, resist cell death, and promote tumour development, progression and invasion.

Our group previously used a Luminex cytokine assay to screen 353 inflammatory factors released by LPS-stimulated macrophages. The most altered cytokines were IL-6, IP10, and TNF-α. Unlike IL-6 and IP10, which have been experimentally demonstrated to promote EBV reactivation by our group, TNF-α significantly inhibited EBV reactivation by acting on the TNFR1 receptor. We experimentally demonstrated that TNF-α had a significant inhibitory effect on EBV reactivation in both LCL and Raji cells. As mentioned above, the regulation of processes such as cell survival and cell death is a hallmark of TNF-α in both inflammatory diseases[27] and cancers[37]. TNF-α has been identified as a major regulator of inflammation and a key player in the cytokine network[38]. TNF-α has contradictory tumour-promoting and tumour-killing effects in cancer therapy[39]. Thus, it

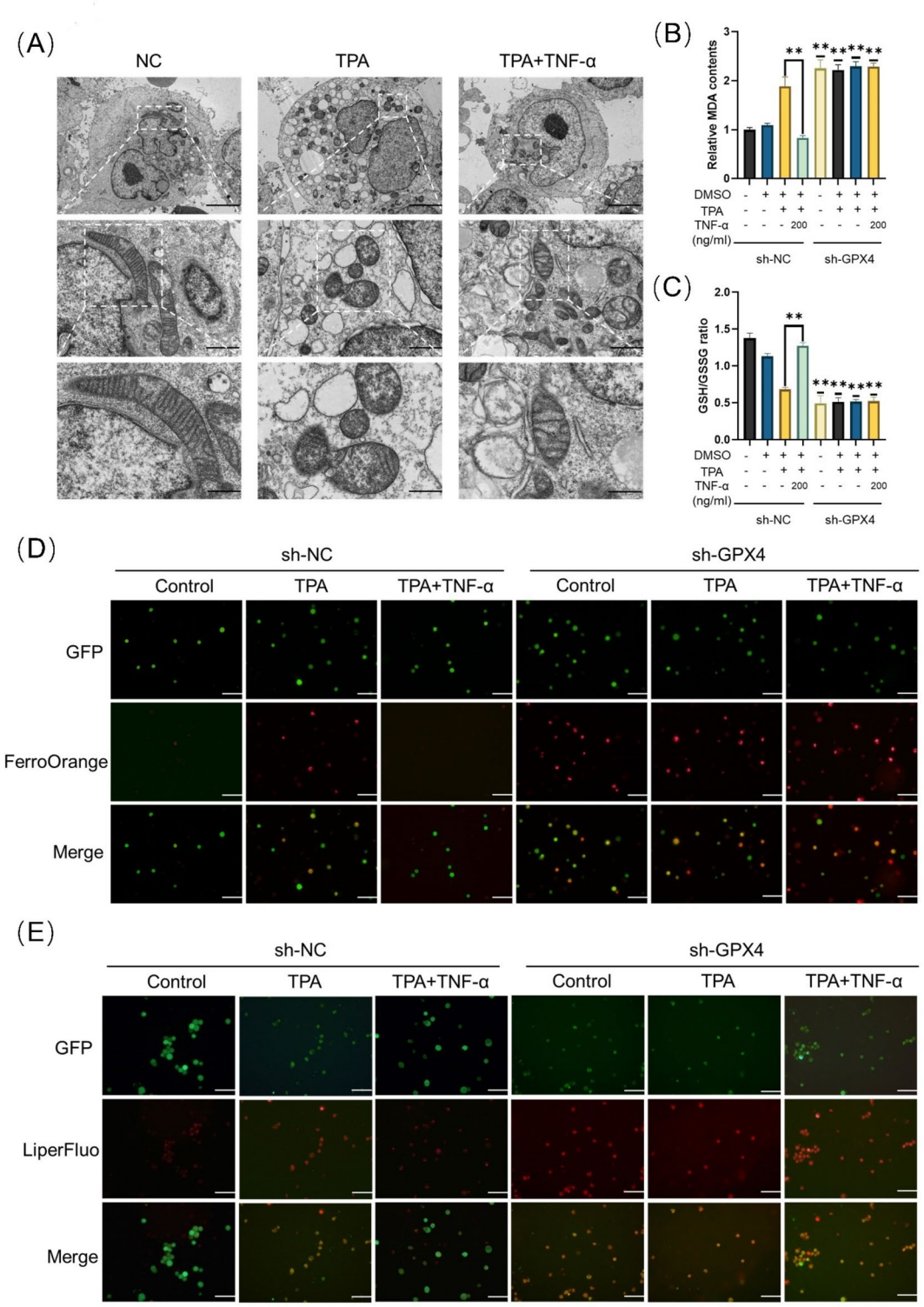

Fig. 4. TNF-α inhibits the EBV reactivation state by affecting latent ferroptosis. (A) Mitochondrial morphology of Raji cells treated with TPA (20 ng/ml) or TNF-α (200 ng/ml) for 24 h was observed using transmission electron microscopy. (B) MDA contents of Raji-shRNA-control and Raji-shRNA-hGPX4-2 cells treated with TPA (20 ng/ml) or TNF-α (200 ng/ml) for 24 h. (C) GSH/GSSG ratios of Raji-shRNA-control and Raji-shRNA-hGPX4-2 cells treated with TPA (20 ng/ml) or TNF-α (200 ng/ml) for 24 h. (D) Intracellular Fe2 + levels were detected in a FerroOrange Assay of Raji-shRNA-control and Raji-shRNA-hGPX4-2 cells, which were treated with TPA (20 ng/ml) and TNF-α (200 ng/ml) for 24 h. GFP indicates the effect of the lentivirus. (E) Lipid ROS levels were analysed using a Liperfluo fluorescence probe in Raji-shRNA-control and Raji-shRNA-hGPX4-2 cells, which were treated with TPA (20 ng/ml) and TNF-α (200 ng/ml) for 24 h. GFP indicates the effect of the lentivirus. The data shown are representative of three independent experiments. The data are presented as the means ± SDs. $^{*}P < 0.05$; $^{**}p < 0.01$ by one-way ANOVA.

is still not clear whether TNF-α is a target or a therapeutic agent for malignant diseases or both[27]. In addition, outside the field of cancer, TNF-α has different effects on different viruses; for example, TNF-α has a significant proviral replicative effect on JC polyomavirus in neuronal tumour cells[40] and has significant antiviral effects on cytomegalovirus CSFV[41], CMV[42] and herpesvirus type I (HSV-1)[43]. TNF-α also acts differently against the same viruses in different cell types. For example, it lacks an antiviral effect on dengue virus in monocyte macrophages[44] and has an antiviral effect on liver cells[45]. As mentioned above, the link between TNF-α and ROS adds another dimension of complexity to the TNF signaling network, as ROS act on numerous proteins required for the regulation of cellular homeostasis, including proteins that mediate cell proliferation, survival, death, differentiation, DNA repair and metabolism[30]. To further investigate the mechanism by which TNF-α inhibits EBV reactivation, we identified the key differential gene GPX4. The inhibition of GPX4 leads to the accumulation of lipid peroxides and the generation of ROS[46]. We experimentally demonstrated that GPX4 plays a key role in EBV reactivation and that the regulation of GPX4 can regulate the EBV latency/cleavage transition. Extensive research has established glutathione peroxidase 4 (GPX4) as a critical regulator in the pathogenesis of multiple pathological conditions, including osteoarthritis[35],cancers[47], and liver disease[48]. We proved that stable endogenous expression of GPX4 maintains the latent state of EBV. If GPX4 expression is reduced, EBV reactivation can result.

The international classification of cell death modalities includes apoptotic and nonapoptotic processes, including necrotic apoptosis, pyroptosis, and ferroptosis. Recent reports suggest a possible link between ferroptosis and EBV reactivation, which is based on the observation of susceptibility to ferroptosis in EBV infections with different levels of activation[20]. Similarly, we enriched the ferroptosis pathway in a KEGG pathway enrichment analysis. In this study, we systematically investigated the role of ferroptosis in human Burkitt's lymphoma cells. The mechanism of EBV reactivation is complex; the process involves multiple factors, including an inflammatory factor storm, cell death, the immune response and oxidative stress. In the cell model, we detected not only Fe2 + accumulation but also a decreased GSH/GSSG ratio and changes in mitochondrial morphology. We also identified the most important antioxidant enzyme and key regulator of ferroptosis, GPX4, a component of System Xc, by TMT proteomics.

As we know, Ferroptosis is regulated mainly by the GSH–GPX4 pathway[49], and we experimentally demonstrated that TNF-α inhibits EBV reactivation by affecting the classical pathway of ferroptosis. The GSH-GPX4 antioxidant system in the mitochondria and cytoplasm is an important mechanism of cellular resistance to ferroptosis. The cystine/glutamate transporter is a heterodimer consisting of disulfide linkages (SLC7A11 and SLC3A2); its main function is the intracellular transfer of cystine into the cell and the extracellular excretion of glutamate. After entering the cell, cystine is oxidized to cysteine, which is ultimately synthesized into glutathione (GSH) by glutathione synthetase and glutamate-cysteine ligase. In addition, with the help of GSH, GPX4 reduces lipid peroxides to lipocalciferol. Several studies have shown that ferroptosis is regulated mainly by the GSH–GPX4 pathway and that GPX4 converts glutathione (GSH) to oxidized glutathione (GSSG)[50]. The inhibition of GPX4 leads to the accumulation of lipid peroxides and the generation of ROS. The ferroptosis signalling pathway is comprehensive, and in addition to the classical disorders of iron metabolism, the glutathione–cysteamine–glutathione system and polyunsaturated fatty acid metabolism, an increasing number of signalling pathways, such as nicotinamide adenine dinucleotide phosphate/ferroptosis-inhibitory protein 1 and tetrahydrobiopterin/GPT cycloheximide 1/dihydrofolate reductase, have been identified[51]. The results of our present study are still limited, as only one of these pathways was verified.

Furthermore, we detected a significant increase in EBV reactivation when a recognized positive inducer of ferroptosis was used, which was completely the opposite of the results when a ferroptosis inhibitor was used. These findings lead to the conclusion that the potential ferroptosis status affects EBV reactivation in cells. Researchers may not be able to conclude that excessive cell death induced by ferroptosis is associated with pathogenic processes based only on the preventive effect of ferrostatin-1 or liproxstatin-1 on cell death[21], as these compounds are essentially antioxidants and may inhibit other ROS-dependent forms of cell death, such as necroptosis[46]. However, different types of cell death usually occur simultaneously during the development of a specific disease. Therefore, we designed in vitro experiments to verify that Fer-1 rescues the EBV reactivation process and showed by electron microscopy that cellular mitochondria undergo morphological changes typical of ferroptosis, which demonstrates the involvement of ferroptosis during EBV reactivation.

Currently, many unresolved issues remain in the field of ferroptosis research. First, there is no gold standard for detecting ferroptosis, especially in the small field of EBV reactivation, where the study of ferroptosis is still in its infancy. Therefore, we can detect only indicators associated with ferroptosis as much as possible. Second, the interactions and translation between ferroptosis and other types of cell death remain unknown. Different types of cell death usually involve similar initial signals and molecular regulators, such as GPX4, which is also involved in apoptosis and necrotic apoptosis in various injuries. To date, there are barely known published studies indicating that GPX4 expression is directly controlled by EBV lytic genes. In our study, we hypothesize a unidirectional relationship between the GSH-GPX4 pathway → ferroptosis → EBV reactivation. We aim to validate this logic through GPX4 protein knockdown and experiments with well-established ferroptosis inducers and inhibitors to demonstrate the cause-and-effect relationship. In our study, we cannot exclude the possibility that EBV reactivation may also influence the GSH-GPX4 pathway. Previous studies have shown that EBV infection reduces the sensitivity of nasopharyngeal carcinoma cells to ferroptosis[52]. However, current research has not provided direct evidence linking EBV lytic genes to the regulation of GPX4 expression. It is plausible that EBV lytic genes, along with the various cellular responses induced during EBV infection, may affect the cellular redox state and antioxidant mechanisms, including the modulation of GPX4 expression. Besides, The mechanisms regulating GPX4 expression are ill-defined[53]. At the level of gene transcription, the fact that three different proteins can be synthesized from gpx4, due to the presence of multiple transcriptional start sites, yielding the mitochondrial (m-), nuclear (n-), and cytosolic (c-) GPx4 forms, makes the issue of gene regulation extremely

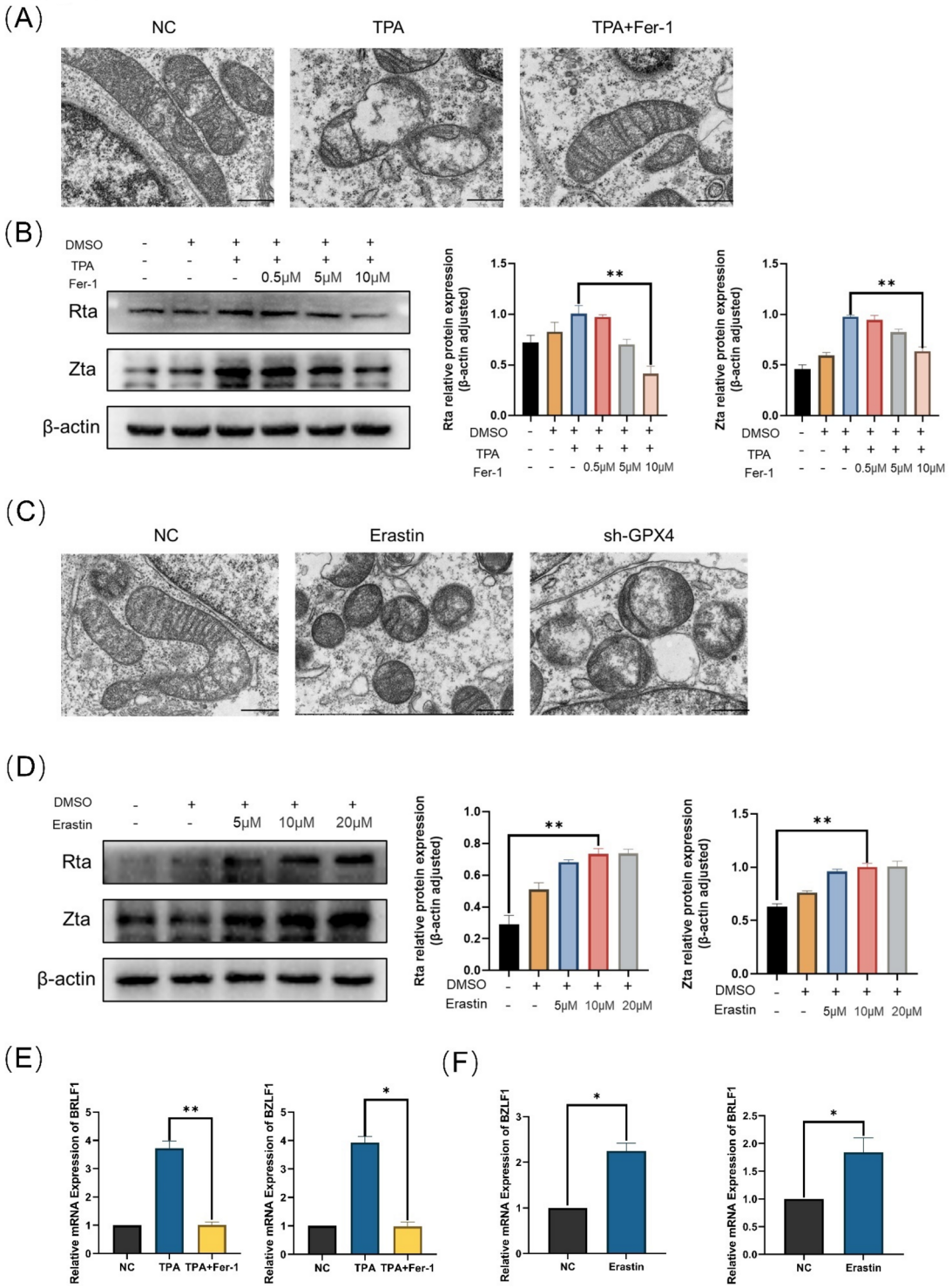

complex[54]. Therefore, it is currently difficult to determine how TNF-α/TNFR1 signaling affects GPX4 expression through transcriptional or post-translational modifications, which relies on further exploration.

Overall, further mechanistic studies are needed in the future to validate the therapeutic potential of TNF-α and the inhibitors and inducers of ferroptosis in EBV-related diseases. In conclusion, we provide some evidence that TNF-α can ultimately inhibit EBV reactivation by affecting GPX protein expression and thereby influencing potential ferroptosis status and ROS. Surprisingly, our results suggest that GPX4 has dual functions in Raji cells: it inhibits cellular activity on the one hand and promotes EBV replication and proliferation on the other hand when GPX4 expression is inhibited. Notably, TNF-α also plays a fascinating dual-sided role, with exogenous TNF-α somewhat rescuing the potential ferroptosis state of the cells caused by TPA while also inhibiting the reactivation of EBV. With the development of assays and methods, additional modes of cell death may be identified in the

◀**Fig. 5**. Ferroptosis Activator (Erastin) and Inhibitor (Fer-1) Promote and Suppress EBV Reactivation. (A) Mitochondrial morphology of Raji cells treated with TPA (20 ng/ml) or Fer-1 (10 μM) for 24 h was observed using transmission electron microscopy. (B) Raji cells were treated with TPA (20 ng/ml) and different concentrations of Fer-1 for 24 h. Western blotting was performed with the indicated antibodies. (C) The mitochondrial morphology of sh-GPX4 group and erastin (10μM) treated group(for 24 h) were observed using transmission electron microscopy. (D) Raji cells were treated with different concentrations of erastin for 24 h. Western blotting was performed with the indicated antibodies. (F) RNA was extracted from Raji cells treated with erastin (10 μM), and the mRNA expression levels of the EBV genes BRLF1 and BZLF1 were measured by real-time PCR. (E) RNA was extracted from Raji cells treated with TPA (20 ng/ml) or Fer-1 (10 μM), and the mRNA expression levels of the EBV genes BRLF1 and BZLF1 were measured by real-time PCR. The data shown are representative of three independent experiments. The data are presented as the means ± SDs. $^{*}P < 0.05$; $^{**}p < 0.01$ by one-way ANOVA.

future. It is critical to understand whether a particular type of cell death occurs during disease progression. Our current study provides a solid foundation for future research on EBV reactivation and ferroptosis.

Materials and methods

Cells and reagents

Raji (Procell) and LCL (Procell) cells were latently infected with EBV. The cells were stored in complete optimal medium (RPMI 1640 + 10% foetal bovine serum). The cells were cultured in a cell incubator at 37 °C, 5% CO2, and 95% humidity. Raji cells and LCL cells were purchased from Procella Life Science & Technology Co., Ltd. Mycoplasma contamination was checked in all used cells.

The following antibodies were used in this study:

mouse monoclonal EBV ZEBRA antibody (sc-53904, Santa Cruz), rabbit polyclonal BRLF1 antibody (bs-45008, Bioss), mouse monoclonal GPX4 antibody (67763-1-Ig, Proteintech), rabbit polyclonal TNFR1 antibody (21574-1-AP; Proteintech), anti-GAPDH rabbit pAb (GB11002, Servicebio), and anti-beta-actin rabbit pAb (GB11001, Servicebio) were used. HRP-conjugated goat anti-rabbit IgG (H + L) and HRP-conjugated goat anti-mouse IgG (H + L) secondary antibodies were purchased from Servicebio. Human TNF-α (PEPROTECH, Cat# 300–01 A), erastin (MCE, HY-15763), R-7050 (MCE, HY-110203), and ferrostatin-1 (MCE, HY-100579) were also purchased.

Western blot analysis

The cells were lysed with lysis buffer (kgp2100, Keygen). The lysate was subsequently centrifuged (12000 × g, 4 °C, 5 min), denatured, analysed by SDS–PAGE, and transferred to PVDF membranes (IPVH15150, Millipore). The PVDF membranes were incubated with primary antibodies overnight at 4 °C, incubated with secondary antibodies at room temperature for 1 h, and visualized using the Bio-Rad ChemiDoc XRS + system. All immunoblotting was repeated at least twice. ImageJ was used for grey value analysis.

RNA extraction and qPCR

RNA was isolated using an RN001 RNA-Quick Purification Kit (ESscience). cDNA was synthesized from 1 g RNA using a fPrime-Script® RT Reagent Kit with gDNAEraser (Takara, Japan). The reactions were carried out on a Bio-Rad CFX ConnectTM Real-Time System. The synthesized cDNA was used as a template for BZRF1 PCR with primers:

forward
5'-CATGTTTCAACCGCTCCGACTGG-3',
reverse
5'-GCGCAGCCTGTCATTTTCAGATG-3';
BRLF1 PCRs with primers:
forward
5'-ACCTCACTACACAAACAGACG-3',
reverse
5'-TGTTGAGGACGTTGCAGTAG-3';
and β-actin PCRs with primers:
forward
5'-CCAAGGCCAACCGCGAGAAGATGAC-3',
reverse
5'-AGGGTACATGGTGGTGCCGCCAGAC-3'.

The thermocycler conditions were 95 °C for 30 s for 1 cycle, 95 °C for 5 s, and 60 °C for 10 s for 40 cycles. Actin was used as an internal control with primers.

EBV DNA extraction and droplet digital PCR of viral DNA

EBV DNA was isolated using a QIAamp DNA Mini kit (51304,QIAGEN) with EBV DNA encapsulated stochastically inside microdroplets as chambers. A small percentage chamber contains one or fewer copies of DNA. After amplification, concentrations were determined based on the proportion of nonfluorescent partitions through the Poisson distribution. The reactions were carried out on a digital PCR machine (D3200).

Immunofluorescence assay

Cells were seeded on coverslips and fixed with 4% paraformaldehyde. After washing with PBS, the coverslips were incubated with 0.5% Triton X-100 for 10 min. The cells were blocked with 5% BSA and then incubated with primary antibodies overnight, followed by incubation with FITC, goat anti-mouse IgG (A22110), DyLight 594, or goat anti-rabbit IgG for 1 h. The cells were then counterstained with DAPI (AR1176, Abbkin) and imaged with fluorescence microscopy.

Apoptosis assay (flow cytometry)

The apoptosis rate of Raji cells was determined by flow cytometry using a dead cell apoptosis kit with Annexin V Alexa Fluor™ 488 and propidium iodide (Invitrogen). The stained cells were analysed using cytoFLEX flow cytometry.

Small interfering RNAs

For the siRNA-mediated knockdown assay, TNFR1 siRNA was purchased from Tsingke Biotechnology. Raji cells were transiently reverse-transfected with siTNFR1 (50 nM), and the cells were cultured for 72 h. Western blotting was performed to determine the effectiveness of the siRNAs. The information on the relevant siRNA sequence is provided below.

Sense (5'-3')
Antisense (5'-3')
si TNFR1 (1)
GAGCUUGAAGGAACUACUA(dT)(dT)
UAGUAGUUCCUUCAAGCUC(dT)(dT)
si TNFR1 (2)
GCUGCAGGAAGAACCAGUA(dT)(dT)
UACUGGUUCUUCCUGCAGC(dT)(dT)
si TNFR1 (3)
CUGUAGUAACUGUAAGAAA(dT)(dT)
UUUCUUACAGUUACUACAG(dT)(dT).

Lentiviral transfection and establishment of stable cell lines

To knock down specific target genes, such as human GPX4 (NM_001039847.3), Raji cells were infected with a lentivirus encoding GPX4 or a control virus. Briefly, according to the manufacturer's protocol, GPX4-knockdown shRNAs were transiently transfected into Raji cells using Lipo8000 reagents (C0533, Beyotime). The MOI value was determined to be 100 in a preexperiment. The cells were cultured for 72 h. Puromycin (A1113803, Life) was used to select chondrocytes in which GPX4 had been stably knocked down.

hGPX4-1-F:
5'-GATCCGTGAGGCAAGACCGAAGTAAACTCGAGTTTACTTCGGTCTTGCCTCACTTTTTG-3'
hGPX4-1-R:
5'-AATTCAAAAAGTGAGGCAAGACCGAAGTAAACTCGAGTTTACTTCGGTCTTGCCTCACG-3'
hGPX4-2-F:
5'-GATCCGGGAGTAACGAAGAGATCAAACTCGAGTTTGATCTCTTCGTTACTCCCTTTTTG-3'
hGPX4-2-R:
5'-AATTCAAAAAGGGAGTAACGAAGAGATCAAACTCGAGTTTGATCTCTTCGTTACTCCCG-3'
hGPX4-3-F:
5'-GATCCACGTCAAATTCGATATGTTCACTCGAGTGAACATATCGAATTTGACGTTTTTTG-3'
hGPX4-3-R:
5'-AATTCAAAAAACGTCAAATTCGATATGTTCACTCGAGTGAACATATCGAATTTGACGTG-3'

Determination of intracellular Fe2+ levels

For Liperfluo staining (Dojindo, Kumamoto, Japan), Raji cells were seeded in a 48-well plate. The cells were treated as described above for 24 h and then stained with Liperfluo (1 mM) for 30 min at 37 °C. After being washed with HBSS, the cells were observed immediately with a fluorescence microscope. Intracellular Fe2 + levels were then determined.

Assessment of lipid peroxidation by liperfluo staining

Raji cells were seeded in a 48-well plate. As described above, the cells were treated for 24 h, washed 3 times in HBSS and stimulated for 20 min in HBSS at 37 °C and 5% CO2. After that, the cells were stained in 1 mM FerroOrange (Dojindo, Kumamoto, Japan) in HBSS for exactly 30 min at 37 °C and 5% CO2 and imaged immediately with a fluorescence microscope.

Bioinformatics analysis

The total protein contents of untreated Raji cells, Raji cells treated with TPA for 24 h and Raji cells treated with TPA and 200 ng/ml TNF-α were analysed by quantitative proteomics. The samples were sent to Sichuan Panomix Biotechnology Ltd. for protein identification. Protein identification analysis was performed on a RIGOLL-3000 high-performance liquid chromatography system (Beijing Puyuan Jingdian Science and Technology Co., Ltd.). The R programming language program was used to analyse the raw data and identify the differentially expressed proteins. Differentially expressed proteins with p values ≤ 0.05 and fold changes ≥ 1 were selected. The list of differentially expressed proteins was then subjected to GO functional enrichment and KEGG pathway enrichment analyses.

Transmission electron microscopy of Raji cells

Untreated Raji cells, Raji cells treated with TPA for 24 h, Raji cells treated with TPA and 200 ng/ml TNF-α, cells treated with 10 μM erastin and 10 μM Fer-1 sh-NC and sh-GPX4 cells were collected and fixed by the addition of electron microscope fixative (G1102 Servicebio) for 2 h at 4 °C. The samples were sent to Wuhan Servicebio Biotechnology Co. for preparation and imaging. Transmission electron microscopy (HT7800 HITACHI) was used for examination.

Measurement of GSH and GSSG

Raji cells were seeded in a 6-well plate. Cells were treated as described above for 24 h. Cells were washed once with PBS, then centrifuge to collect the cells and discard the supernatant. Add three times the volume of protein removal reagent M to the cell pellet and vortex thoroughly. Perform two cycles of rapid freezing and thawing using liquid nitrogen and a 37°C water bath. Incubate the sample on ice at 4°C for 5 minutes. Finally, centrifuge at 10,000 g for 10 minutes at 4°C and collect the supernatant for total glutathione measurement. The supernatant was collected, and the total GSH and GSSG levels were determined by GSH and GSSG Assay Kit (Beyotime, Jiangsu, China) following the manufacturer' instruction.

Intracellular ROS detection

Intracellular ROS content was measured by the flow cytometry or microplate reader utilizing DCFH-DA. Raji cells were seeded in a 6-well plate. In the day of the experiment, cells were stained with 10 μM DCFH-DA at 37 °C for 30 min, then were treated as described above for 4 h. Cells were harvested and analyzed by the flow cytometry or microplate reader (Ex/Em = 488 nm/525 nm).

(Beyotime, Jiangsu, China)

Malondialdehyde (MDA) assay

MDA content was measured by Lipid Peroxidation MDA Assay Kit (Beyotime, Jiangsu, China). Raji cells were seeded in a 6-well plate. Cells were treated as described above for 24 h. Protein lysates were harvested using Cell Lysis Buffer supplemented with Protease Inhibitor. 200 μl MDA detection working buffer was added into 100 μl samples or standard solution, which was followed by heat in 100 °C hot iron block for 15 min and water bath cooling to room temperature Then the tubes were centrifuged at 1000 x g at room temperature for 10 min and measured the absorbance of A532. The protein concentrations were quantified using a BCA Protein Assay Kit (Thermo, Waltham, USA)to normalize the MDA content.

Enzyme-Linked immunosorbent assay (ELISA)

Prepare the working solutions according to the kit instructions. Set up the standard, zero, blank, and sample wells, adding the appropriate volumes of standards, sample dilution buffer, and test samples. Add 100μL of HRP-labeled detection antibody to all wells except the blank well. Incubate at 37 °C for 60 min, protected from light. After incubation, wash the wells 5 times with washing buffer, blot dry, and add 100μL of a 1:1 mixture of substrate A and B to each well. Incubate at 37 °C for 15 min, protected from light. Finally, add 50μL of stop solution to each well and read the absorbance (OD value) at 450 nm using a microplate reader. (RX104793H,96T RUIXIN BIOTECH)

Statistical analysis

All the results are presented as the means ± standard deviations (means ± SDs). Statistical analyses were performed with GraphPad Prism. Unpaired Student's t test (for two groups) and one-way or two-way ANOVA (for multiple groups) were used, followed by the Tukey–Kramer test ($^{*}p < 0.05$ was considered statistically significant, $^{**}p < 0.01$, $^{***}p < 0.001$).

Data availability

All data generated or analysed during this study are included in this published article [and its supplementary information files].

Received: 17 October 2024; Accepted: 14 April 2025
Published online: 12 May 2025

References

1. Young, L. S., Yap, L. F. & Murray, P. G. Epstein–Barr virus: more than 50 years old and still providing surprises. *Nat. Rev. Cancer.* **16** (12), 789–802. https://doi.org/10.1038/nrc.2016.92 (2016).
2. Münz, C. Latency and lytic replication in Epstein–Barr virus-associated oncogenesis. *Nat. Rev. Microbiol.* **17** (11), 691–700. https://doi.org/10.1038/s41579-019-0249-7 (2019).
3. Kerr, J. R. Epstein-Barr virus (EBV) reactivation and therapeutic inhibitors. *J. Clin. Pathol.* **72** (10), 651–658. https://doi.org/10.1136/jclinpath-2019-205822 (2019).
4. Houen, G. & Trier, N. H. Epstein-Barr virus and systemic autoimmune diseases. *Front. Immunol.* **11**, 587380. https://doi.org/10.3389/fimmu.2020.587380 (2021).
5. Chene, A. et al. Endemic Burkitt's lymphoma as a polymicrobial disease. *Sem. Cancer Biol.* **19** (6), 411–420. https://doi.org/10.1016/j.semcancer.2009.10.002 (2009).
6. Chen, Y. P. et al. Nasopharyngeal carcinoma. *Lancet* **394** (10192), 64–80. https://doi.org/10.1016/S0140-6736(19)30956-0 (2019).
7. Hu, J. et al. Targeting Epstein-Barr virus oncoprotein LMP1-mediated high oxidative stress suppresses EBV lytic reactivation and sensitizes tumors to radiation therapy. *Theranostics* **10** (26), 11921–11937. https://doi.org/10.7150/thno.46006 (2020).
8. Cui, X. & Snapper, C. M. Epstein barr virus: development of vaccines and immune cell therapy for EBV-Associated diseases. *Front. Immunol.* https://doi.org/10.3389/fimmu.2021.734471 (2021).

9. Su, Y. et al. Multiple early factors anticipate post-acute COVID-19 sequelae. *Cell* **185** (5), 881–895e20. https://doi.org/10.1016/j.cell.2022.01.014 (2022).
10. Zhang, H. et al. HDAC2 is required by the physiological concentration of glucocorticoid to inhibit inflammation in cardiac fibroblasts. *Can. J. Physiol. Pharmacol.* **95** (9), 1030–1038. https://doi.org/10.1139/cjpp-2016-0449 (2017).
11. Fernandez, S. G. & Miranda, J. L. Bendamustine reactivates latent Epstein-Barr virus. *Leuk. Lymphoma.* **57** (5), 1208–1210. https://doi.org/10.3109/10428194.2015.1079317 (2016).
12. Liu, S. F. et al. Aspirin induces lytic cytotoxicity in Epstein–Barr virus-positive cells. *Eur. J. Pharmacol.* **589** (1–3), 8–13. https://doi.org/10.1016/j.ejphar.2008.04.025 (2008).
13. Wang, Y. et al. IL-21 stimulates the expression and activation of cell cycle regulators and promotes cell proliferation in EBV-positive diffuse large B cell lymphoma. *Sci. Rep.* **10**, 12326. https://doi.org/10.1038/s41598-020-69227-0 (2020).
14. Li, H. et al. Epstein-Barr virus lytic reactivation regulation and its pathogenic role in carcinogenesis. *Int. J. Biol. Sci.* **12** (11), 1309–1318. https://doi.org/10.7150/ijbs.16564 (2016).
15. Li, Y. et al. Epstein-Barr virus BZLF1-mediated downregulation of proinflammatory factors is essential for optimal lytic viral replication. (Longnecke,r R.M. ed.) *J. Virol.* **90**(2), 887–903 (2016). https://doi.org/10.1128/JVI.01921-15
16. Bernaudat, F. et al. Structural basis of DNA methylation-dependent site selectivity of the Epstein–Barr virus lytic switch protein ZEBRA/Zta/BZLF1. *Nucleic Acids Res.* **50** (1), 490–511. https://doi.org/10.1093/nar/gkab1183 (2022).
17. Huang, S. Y. et al. Reactive oxygen species mediate Epstein-Barr virus reactivation by N-Methyl-N'-Nitro-N-Nitrosoguanidine (Masucci MG, ed.). *PLoS ONE.* **8** (12), e84919. https://doi.org/10.1371/journal.pone.0084919 (2013).
18. Zhang, S., Yin, J. & Zhong, J. Chaetocin reactivates the lytic replication of Epstein-Barr virus from latency via reactive oxygen species. *Sci. China Life Sci.* **60** (1), 66–71. https://doi.org/10.1007/s11427-016-0286-7 (2017).
19. Zhao, L. et al. Chlorpyrifos induces the expression of the Epstein-Barr virus lytic cycle activator BZLF-1 via reactive oxygen species. *Oxidative Med. Cell. Longev.* **2015** (1), 309125. https://doi.org/10.1155/2015/309125 (2015).
20. Burton, E. M., Voyer, J. & Gewurz, B. E. Epstein–Barr virus latency programs dynamically sensitize B cells to ferroptosis. *Proc. Natl. Acad. Sci. U S A.* **119** (11), e2118300119. https://doi.org/10.1073/pnas.2118300119 (2022).
21. Stockwell, B. R. et al. Ferroptosis: A regulated cell death Nexus linking metabolism, redox biology, and disease. *Cell* **171** (2), 273–285. https://doi.org/10.1016/j.cell.2017.09.021 (2017).
22. Sun, Y. et al. The emerging role of ferroptosis in inflammation. *Biomed. Pharmacother.* **127**, 110108. https://doi.org/10.1016/j.biopha.2020.110108 (2020).
23. Ferroptosis: Molecular mechanisms and health implications. *Cell Res*. https://www.nature.com/articles/s41422-020-00441-1. Accessed 24 June 2024.
24. Heikkilä, O., Nygårdas, M., Paavilainen, H., Ryödi, E. & Hukkanen, V. Interleukin-27 inhibits herpes simplex virus type 1 infection by activating STAT1 and 3, Interleukin-6, and chemokines IP-10 and MIG. *J. Interferon Cytokine Res.* **36** (11), 617–629. https://doi.org/10.1089/jir.2016.0015 (2016).
25. Reese, T. A. et al. Helminth infection reactivates latent g-herpesvirus via cytokine competition at a viral promoter. https://doi.org/10.1126/science.1254517
26. Chen, G. & Goeddel, D. V. TNF-R1 signaling: A beautiful pathway. *Science* **296** (5573), 1634–1635. https://doi.org/10.1126/science.1071924 (2002).
27. van Loo, G. & Bertrand, M. J. M. Death by TNF: a road to inflammation. *Nat. Rev. Immunol.* **23** (5), 289–303. https://doi.org/10.1038/s41577-022-00792-3 (2023).
28. Liao, Y. et al. Oral microbiota alteration and roles in Epstein-Barr Virus reactivation in nasopharyngeal carcinoma (Li, J. ed.) *Microbiol. Spectr.* **11**(1), e03448-22 (2023). https://doi.org/10.1128/spectrum.03448-22
29. Baran-Marszak, F. et al. Effect of tumor necrosis factor alpha and Infliximab on apoptosis of B lymphocytes infected or not with Epstein–Barr virus. *Cytokine* **33** (6), 337–345. https://doi.org/10.1016/j.cyto.2006.03.005 (2006).
30. Aggarwal, B. B., Gupta, S. C. & Kim, J. H. Historical perspectives on tumor necrosis factor and its superfamily: 25 years later, a golden journey. *Blood* **119** (3), 651–665. https://doi.org/10.1182/blood-2011-04-325225 (2012).
31. Blaser, H., Dostert, C., Mak, T. W. & Brenner, D. TNF and ROS crosstalk in inflammation. *Trends Cell Biol.* **26** (4), 249–261. https://doi.org/10.1016/j.tcb.2015.12.002 (2016).
32. Miyauchi, K., Urano, E., Yoshiyama, H. & Komano, J. Cytokine signatures of transformed B cells with distinct Epstein–Barr virus latencies as a potential diagnostic tool for B cell lymphoma. *Cancer Sci.* **102** (6), 1236–1241. https://doi.org/10.1111/j.1349-7006.2011.01924.x (2011).
33. Fitzsimmons, L. & Kelly, G. L. EBV and apoptosis: the viral master regulator of cell fate?? *Viruses* **9** (11), 339. https://doi.org/10.3390/v9110339 (2017).
34. Hou, L., Huang, R., Sun, F., Zhang, L. & Wang, Q. NADPH oxidase regulates Paraquat and maneb-induced dopaminergic neurodegeneration through ferroptosis. *Toxicology* **417**, 64–73. https://doi.org/10.1016/j.tox.2019.02.011 (2019).
35. Miao, Y. et al. Contribution of ferroptosis and GPX4's dual functions to osteoarthritis progression. *eBioMedicine* **76**, 103847. https://doi.org/10.1016/j.ebiom.2022.103847 (2022).
36. Saito, M. & Kono, K. Landscape of EBV-positive gastric cancer. *Gastric Cancer.* **24** (5), 983–989. https://doi.org/10.1007/s10120-021-01215-3 (2021).
37. Balkwill, F. Tumour necrosis factor and cancer. *Nat. Rev. Cancer.* **9** (5), 361–371. https://doi.org/10.1038/nrc2628 (2009).
38. Lin, S. Y. et al. TNF-α receptor inhibitor alleviates metabolic and inflammatory changes in a rat model of ischemic stroke. *Antioxid. (Basel).* **10** (6), 851. https://doi.org/10.3390/antiox10060851 (2021).
39. Cruceriu, D., Baldasici, O., Balacescu, O. & Berindan-Neagoe, I. The dual role of tumor necrosis factor-alpha (TNF-α) in breast cancer: molecular insights and therapeutic approaches. *Cell. Oncol.* **43** (1), 1–18. https://doi.org/10.1007/s13402-019-00489-1 (2020).
40. Nukuzuma, S. et al. TNF-α stimulates efficient JC virus replication in neuroblastoma cells: TNF-α stimulates replication of JC virus. *J. Med. Virol.* **86** (12), 2026–2032. https://doi.org/10.1002/jmv.23886 (2014).
41. Liniger, M., Gerber, M., Renzullo, S., García-Nicolás, O. & Ruggli, N. TNF-Mediated Inhibition of classical swine fever virus replication is IRF1-, NF-κB- and JAK/STAT Signaling-Dependent. *Viruses* **13** (10), 2017. https://doi.org/10.3390/v13102017 (2021).
42. Montag, C. et al. The latency-associated UL138 gene product of human cytomegalovirus sensitizes cells to tumor necrosis factor alpha (TNF-α) signaling by upregulating TNF-α receptor 1 cell surface expression. *J. Virol.* **85**. https://doi.org/10.1128/JVI.05028-11 (2011).
43. Cai, M. et al. Herpes simplex virus 1 UL2 inhibits the TNF-α–Mediated NF-κB activity by interacting with p65/p50. *Front. Immunol.* **11**, 549. https://doi.org/10.3389/fimmu.2020.00549 (2020).
44. Wati, S. et al. Tumour necrosis factor alpha (TNF-) stimulation of cells with established dengue virus type 2 infection induces cell death that is accompanied by a reduced ability of TNF- to activate nuclear factor B and reduced sphingosine kinase-1 activity. *J. Gen. Virol.* **92** (4), 807–818. https://doi.org/10.1099/vir.0.028159-0 (2011).
45. Wati, S., Li, P., Burrell, C. J. & Carr, J. M. Dengue virus (DV) replication in Monocyte-Derived macrophages is not affected by tumor necrosis factor alpha (TNF-α), and DV infection induces altered responsiveness to TNF-α stimulation. *J. Virol.* **81** (18), 10161–10171. https://doi.org/10.1128/JVI.00313-07 (2007).
46. Jiang, X., Stockwell, B. R. & Conrad, M. Ferroptosis: mechanisms, biology and role in disease. *Nat. Rev. Mol. Cell. Biol.* **22** (4), 266–282. https://doi.org/10.1038/s41580-020-00324-8 (2021).

47. Huang, S. et al. Induction of ferroptosis in human nasopharyngeal cancer cells by cucurbitacin B: molecular mechanism and therapeutic potential. *Cell. Death Dis.* **12** (3), 237. https://doi.org/10.1038/s41419-021-03516-y (2021).
48. Chen, J., Li, X., Ge, C., Min, J. & Wang, F. The multifaceted role of ferroptosis in liver disease. *Cell. Death Differ.* **29** (3), 467–480. https://doi.org/10.1038/s41418-022-00941-0 (2022).
49. Dixon, S. J. & Olzmann, J. A. The cell biology of ferroptosis. *Nat. Rev. Mol. Cell. Biol.* **25** (6), 424–442. https://doi.org/10.1038/s41580-024-00703-5 (2024).
50. Wu, K. et al. Creatine kinase B suppresses ferroptosis by phosphorylating GPX4 through a moonlighting function. *Nat. Cell. Biol.* **25** (5), 714–725. https://doi.org/10.1038/s41556-023-01133-9 (2023).
51. Wang, Y., Yan, D., Liu, J., Tang, D. & Chen, X. Protein modification and degradation in ferroptosis. *Redox Biol.* **75**, 103259. https://doi.org/10.1016/j.redox.2024.103259 (2024).
52. Yuan, L. et al. EBV infection-induced GPX4 promotes chemoresistance and tumor progression in nasopharyngeal carcinoma. *Cell. Death Differ.* **29** (8), 1513–1527. https://doi.org/10.1038/s41418-022-00939-8 (2022).
53. Ursini, F. & Maiorino, M. Lipid peroxidation and ferroptosis: the role of GSH and GPx4. *Free Radic. Biol. Med.* **152**, 175–185. https://doi.org/10.1016/j.freeradbiomed.2020.02.027 (2020).
54. Distinct Promoters Determine. Alternative transcription of gpx-4 into Phospholipid-Hydroperoxide glutathione peroxidase variants. *J. Biol. Chem.* **278** (36), 34286–34290. https://doi.org/10.1074/jbc.M305327200 (2003).

Author contributions
The project was designed by LYG, LYH and ZYY. ZYY and LYG conceived and designed the experiments. ZYY, WYL, DBN, LQ, CXN, XMY, LHL performed the experiments. ZYY analysed the data. ZYY wrote the paper. LYG, LYH and WYL reviewed and modified the manuscript. All the authors contributed to the paper and approved the submitted version.

Funding
This study was supported by the Natural Science Foundation of Chongqing (grant no. cstc2021jcyj-msxmX0306).

Declarations

Competing interests
The authors declare no competing interests.

Additional information
Supplementary Information The online version contains supplementary material available at https://doi.org/10.1038/s41598-025-98679-5.

Correspondence and requests for materials should be addressed to Y.L. or Y.L.